Pergamon

Tetrahedron Letters 42 (2001) 7997–8001

TETRAHEDRON LETTERS

Tetra-*tert*-butyl-*as*-indaceno[1,2,3-*cd*:6,7,8-*c′d′*]diphenalene: a four-stage amphoteric redox system†

Takashi Kubo,[a] Kagetoshi Yamamoto,[a,*] Kazuhiro Nakasuji[a,*] and Takeji Takui[b]

[a]*Department of Chemistry, Graduate School of Science, Osaka University, Toyonaka 560-0043, Japan*
[b]*Department of Chemistry, Faculty of Science, Osaka City University, Sumiyoshi-ku 558-8585, Japan*

Received 9 August 2001; accepted 21 August 2001

Abstract—Tetra-*tert*-butyl-*as*-indaceno[1,2,3-*cd*:6,7,8-*c′d′*]diphenalene (TTB-*as*-IDPL) was prepared and found to behave as a four-stage amphoteric redox compound. The properties of its five redox states were investigated.

Recently, we have reported the properties of TTB-IDPL **1b** as a four-stage amphoteric redox compound.[1] The compound *as*-IDPL **2a** is an isomer of IDPL **1a**, consisting of two phenalenyl units and an unstable *as*-indacene unit instead of the *s*-indacene unit incorporated in **1a** (Fig. 1). Since both the phenalenyl and *s*-indaceno units play an important role for the characteristic properties of IDPL, *as*-IDPL is also expected to show high amphotericity and to behave as a four-stage amphoteric redox system (Fig. 2). However, the lowered symmetry from D_{2h} to C_{2v} may be related to the different electronic features between IDPL and *as*-IDPL. These ideas are supported by the HMO calculations indicating (a) the smaller HOMO–LUMO energy gap than that of **1a**, then smaller E_1^{sum} value,[2] (b) the LUMO with no longer maintaining the NBMO character becomes weakly bonding (Fig. 3). These considerations prompted us to investigate the chemistry of *as*-IDPL. Herein, we describe the synthesis of the title compound and its properties.

The synthesis of **2b** was summarized in Scheme 1.[3] The compounds **4**–**11** were obtained as a mixture of regioisomers with difficult separation; one isomer is shown in each compound. The reaction of **11** with an equimolar *p*-chloranil afforded the target hydrocarbon **2b** as a greenish-brown oil. The hydrocarbon **2b** was found to be extremely air-sensitive compared to **1b**. The compound **2b** decomposed for 5 h in the air, while **1b**

$$\mathbf{2}^{2+} \underset{-e^-}{\overset{+e^-}{\rightleftharpoons}} \mathbf{2}^{\bullet+} \underset{-e^-}{\overset{+e^-}{\rightleftharpoons}} \mathbf{2} \underset{-e^-}{\overset{+e^-}{\rightleftharpoons}} \mathbf{2}^{\bullet-} \underset{-e^-}{\overset{+e^-}{\rightleftharpoons}} \mathbf{2}^{2-}$$

Figure 2. Four-stage amphoteric redox behavior of **2**.

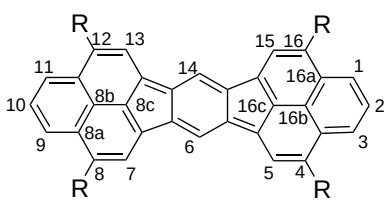

1a R = H, **1b** R = ^{t}Bu

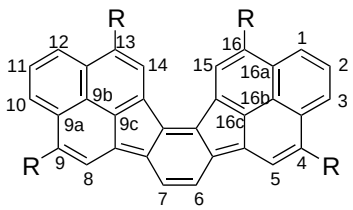

2a R = H, **2b** R = ^{t}Bu

α-position: 1,3,4,5a,7b,9,10,12,13,14a,14d,16
β-position: 2,5,8,11,14,15

Figure 1.

Keywords: amphoteric redox; phenalenyl; ring current; π-spin density.

* Corresponding authors. Fax: +81 6 6850 5395; e-mail: yamamoto@chem.sci.osaka-u.ac.jp; nakasuji@chem.sci.osaka-u.ac.jp

† This paper is dedicated to Emeritus Professor Masazumi Nakagawa on the occasion of his 85th birthday.

0040-4039/01/$ - see front matter
PII: S0040-4039(01)01565-9

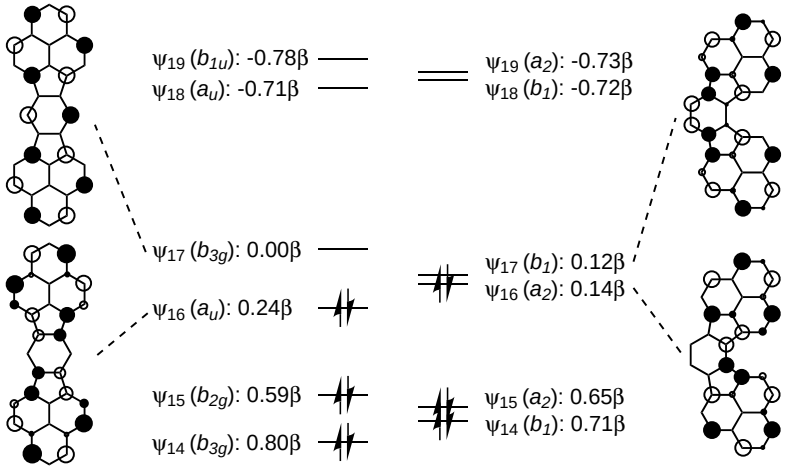

Figure 3. Selected molecular orbitals of **1a** and **2a** calculated by the HMO method.

was stable for several weeks. However, **2b** exhibited no decomposition for a day under vacuum. The FAB MS (NBA) spectra supported the generation of **2b** to give a peak at m/z 624 (M^+) with an unexpected additional peak at m/z 640, probably arising from the oxidation of **2b**. The ^1H NMR spectra gave no useful information about the structure of **2b** due to the absence of signals in the aromatic regions, and showed only broad peaks at 1–2 ppm even at –90°C. Dissolution of **2b** in D_2SO_4 gave simple ^1H and ^{13}C NMR spectra, which was assignable to signals of $\mathbf{2b}^{2+}$. Furthermore, oxidation of **2b** with $SbCl_5$ provided the electronic spectrum identical with that of $\mathbf{2b}^{2+}$ in H_2SO_4. These observations also supported the formation of **2b** by the dehydration of **11**.

The vivid green color TTB-IDPL **1b** shows a simple electronic absorption spectrum, the simplicity of which may be ascribed to the fact that allowed-transitions change to forbidden-ones due to the high symmetry. In contrast with **1b**, TTB-*as*-IDPL **2b** with a dark greenish-brown color gave the complicated UV spectrum as expected. The lower symmetry of **2b** would cause changes from the forbidden to allowed transitions and give rise to many transitions in the UV spectrum. The weak terminal absorption at 1242 nm can be assigned to the HOMO–LUMO transition on the basis of INDO/S calculations.

The cyclic voltammogram of **2b** exhibited four reversible redox waves, providing evidence for the for-

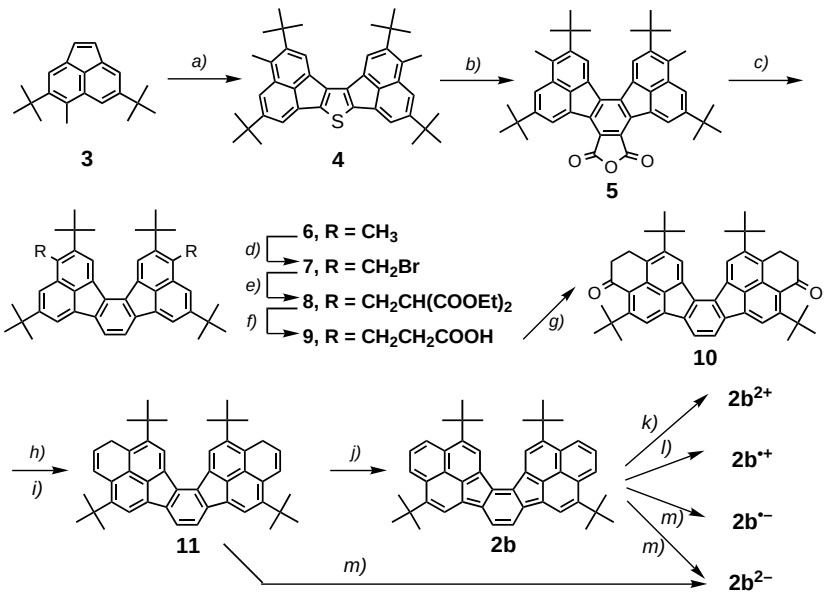

Scheme 1. *Reagents and conditions*: (a) S_8, DMF, 135°C, 3 h, 65%; (b) maleic anhydride, 225°C, 30 min, 79%; (c) basic $CuCO_3$, quinoline, reflux, 6 h, 75%; (d) NBS, benzoyl peroxide, benzene, reflux, 10 min; (e) NaOEt, $CH_2(COOEt)_2$, EtOH–benzene, rt, 1 day, 62% (two steps); (f) (1) aqueous KOH, EtOH, reflux, 3 h, (2) 4N HCl, (3) reflux, H_2O, 8 h, 91%; (g) (1) $(COCl)_2$, reflux, 2 h, (2) $AlCl_3$, CH_2Cl_2, –40°C, 3 h, 80%; (h) LAH, THF, rt, 1 h, 97%; (i) cat. *p*-toluenesulfonic acid, benzene, reflux, 3 min, 90%; (j) *p*-chloranil, benzene, reflux, 5 min; (k) D_2SO_4 or excess $SbCl_5$, CH_2Cl_2; (l) 1 equiv. $SbCl_5$, CH_2Cl_2; (m) K-mirror, under vacuum, THF.

mation of the stable singly and doubly charged species. TTB-*as*-IDPL **2b** behaves, as expected, as a four-stage amphoteric redox compound. Table 1 lists the electrochemical data for **2b** along with those for **1b**. The oxidation potentials (E_1^{ox} and E_2^{ox}) of **2b** appear in more negative regions than those of **1b**. In contrast, the reduction potentials (E_1^{red} and E_2^{red}) of **2b** are more positive than those of **1b**. Compared to **1b**, the higher oxidation and reduction ability of **2b** causes the smaller E_1^{sum} (1.00 V) and E_2^{sum} (1.71 V). The E_1^{sum} of **2b** is comparable to that of PDPL with the smallest E_1^{sum} (0.99 V) among the closed-shell hydrocarbons,[4] whereas the E_2^{sum} of **2b** is the smallest value among them. These findings are consistent with the expectation based on the HMO calculations.

The following consideration may account for the smaller E_1^{sum} and the instability of **2b**. As shown in Fig. 4, the frontier orbital distributions of the central indacene units of **1a** and **2a** are similar to those of *s*- and *as*-indacene, respectively, and those of phenalenyl units are almost the same among HOMO and LUMO of **1a** and **2a**. These MO distributions suggest that the difference in the redox abilities between **1a** and **2a** mainly depends on the central indacene units. On the basis of the HMO calculation, *as*-indacene has a smaller HOMO–LUMO gap than that of *s*-indacene. This feature of *as*-indacene may reflect the smaller HOMO–LUMO gap of **2b**, which was evidenced by the electronic spectrum and the cyclic voltammogram. The smaller energy gap of **2b** causes the larger extent of biradicaloid character, which leads to the fact that **2b** is kinetically less stable than **1b**.

Formation of the stable singly and doubly charged species is summarized in Scheme 1. Dissolution of **2b** in concentrated D_2SO_4 gave the dication species $\mathbf{2b}^{2+}$ as a red–purple solution. Treatment of the dihydro compounds **3** or **2b** with a potassium mirror in degassed THF-d_8 in a sealed tube at −78°C yielded the dianion species $\mathbf{2b}^{2-}$ as a deep yellowish–red solution with yellow fluorescence.

Table 1. CV data (V versus SCE) of **2b** and **1b**

	E_2^{ox}	E_1^{ox}	E_1^{red}	E_2^{red}	E_1^{sum}	E_2^{sum}
2b	+0.75	+0.42	−0.58	−0.96	1.00	1.71
1b	+0.84	+0.48	−0.67	−1.25	1.16	2.09

Measured in dichloromethane with 0.1 M $(^nBu)_4NClO_4$ as supporting electrolyte at room temperature; sweep rate = 100 mV/s.

The ^1H and ^{13}C NMR chemical shifts for $\mathbf{2b}^{2+}$ and $\mathbf{2b}^{2-}$ are given in Table 2. The ^{13}C NMR spectra reveals only minor differences in the chemical shifts in comparison with those of $\mathbf{1b}^{2+}$ and $\mathbf{1b}^{2-}$. The ^{13}C chemical shift changes in the sp^2 carbons on going from $\mathbf{2b}^{2+}$ to $\mathbf{2b}^{2-}$ add up to 725.68 ppm (or 181.42 ppm per electron), supporting the complete generation of the dication and the dianion.[5] The shift changes in the individual carbons for **2b** are similar to those for **1b**; large at the

Table 2. ^1H and ^{13}C NMR data (δ) of $\mathbf{2b}^{2+}$ and $\mathbf{2b}^{2-}$, and ^{13}C chemical shift changes on going from $\mathbf{2b}^{2+}$ to $\mathbf{2b}^{2-}$

Position	$\mathbf{2b}^{2+}$		$\mathbf{2b}^{2-}$		[a]	$\Delta\delta_c$[b]
	^1H	^{13}C	^1H	^{13}C		
1, 12	9.3	147.4	8.02	114.5	α	32.9
2, 11	7.9	131.0	7.55	119.8	β	11.2
3, 10	9.31	149.0	8.02	114.8	α	34.2
4, 9		183.7		128.2	α	55.5
5, 8	7.95	122.8	8.52	116.2	β	6.6
6, 7	7.37	132.3	8.44	110.4		21.9
13, 16		181.9		128.3	α	53.6
14, 15	8.32	126.2	9.4	121.6	β	4.6
5a, 7b		157.9		112.9	α	45
14a, 14d		154.8		112.2	α	42.6
14b, 14c		143.1		121.5		21.6
5b, 7a		147.1		122.4		24.7
12a, 16a		133.4		131.6		1.8
9b, 16b		126.9		130.1		−3.2
9c, 16c		135.3		128.2		7.1
3a, 9a		133.4		131.5		1.9

$\mathbf{2b}^{2+}$, recorded in D_2SO_4 at room temperature. $\mathbf{2b}^{2-}$, recorded in THF-d_8 at room temperature.

[a] Character of positions; α indicates positions with larger charge distributions calculated, β indicates positions with smaller charge distributions calculated.

[b] $\Delta\delta = {}^{13}C(\mathbf{2b}^{2+}) - {}^{13}C(\mathbf{2b}^{2-})$.

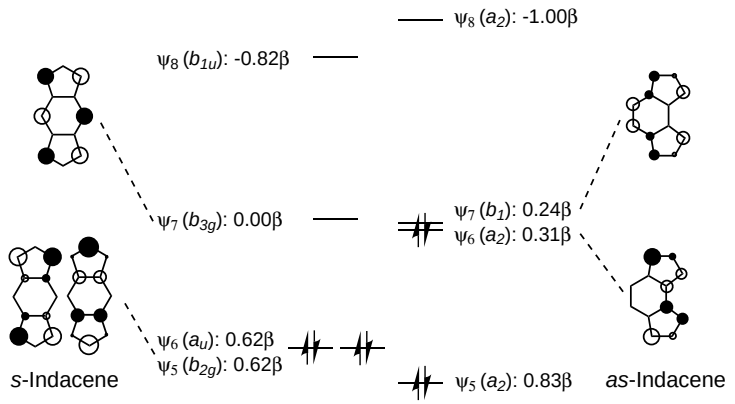

Figure 4. Selected molecular orbitals of *s*-indacene and *as*-indacene calculated by the HMO method.

α-position and the central benzene ring, and small at the others. Charge distributions on the phenalenyl units for $\mathbf{2b}^{2+}$ and $\mathbf{2b}^{2-}$ are similar to those for phenalenyl ions.[6] Furthermore, the HMO calculation indicates 89% of the total positive charges and 78% of the total negative charges on two phenalenyl units in the dication and dianion states, respectively. These findings suggest the large contribution of the phenalenyl units to the stability of $\mathbf{2b}^{2+}$ and $\mathbf{2b}^{2-}$. In contrast, ^{1}H NMR exhibited large differences in the chemical shifts between $\mathbf{2b}^{2+}$ and $\mathbf{1b}^{2+}$. The ring protons of $\mathbf{2b}^{2+}$ are more deshielded by about 0.5 ppm than those of $\mathbf{1b}^{2+}$ except for H_{14} and H_{15}, which move to more downfield by the steric compression effect. The ring current calculation for $\mathbf{2a}^{2+}$ indicates the more weakly paramagnetic ring current on the *as*-indacene unit and the more strongly diatropic ring current on the two phenalenyl units than those of $\mathbf{1a}^{2+}$ (Fig. 5).[7] These ring current effects can explain the more deshielded proton signals of $\mathbf{2b}^{2+}$ than those of $\mathbf{1b}^{2+}$. The ^{1}H signals of $\mathbf{2b}^{2-}$ also appear in a more down-field region than those of $\mathbf{1b}^{2-}$ except for H_6 and H_7, which are central benzene ring protons. These down-field shifts are consistent with the ring current calculation for $\mathbf{2a}^{2-}$, which shows the more strongly diatropic ring currents on the phenalenyl and the cyclopentadienyl units, and less diatropic ring currents on central benzene ring in comparison with $\mathbf{1a}^{2-}$.

The reaction of **2b** with $SbCl_5$ in CH_2Cl_2 generated the radical cation $\mathbf{2b}^{\bullet+}$. The radical anion $\mathbf{2b}^{\bullet-}$ was obtained by the treatment of **2b** with a K-mirror in THF. The both radical species were stable even at room temperature. These species gave rise to the well-resolved ESR spectra with no detectable changes in the range of 213–273 K. The experimental coupling constants of the ring protons for $\mathbf{2b}^{\bullet+}$ and $\mathbf{2b}^{\bullet-}$ are given in Table 3 along with the theoretical ones calculated by the HMO–McLachlan method ($\lambda = 1.2$).[8] The assignment of the coupling constants is based on the calculated coupling constants, although the relatively small magnitudes of $a_{H\mu}$ were somewhat obscure. Studies of the radical cation of the 2,10-dideuterated derivatives **2b** permitted assignment for the constants of H_2 and H_{11}. In both radical species, the large coupling constants can be assigned to the α-positions, and the small ones to the β-positions; these are comparable to those of the radical ions of **1b**. However, the uncertain assignment of the small coupling constants at the β-positions precluded detailed discussion of the electronic states of $\mathbf{2b}^{\bullet+}$ and $\mathbf{2b}^{\bullet-}$. The HMO–McLachlan calculation shows that 87 and 77% of the π-spin reside on the two phenalenyl units in $\mathbf{2b}^{\bullet+}$ and $\mathbf{2b}^{\bullet-}$, respectively. Although π-spin density on the phenalenyl units of $\mathbf{2b}^{\bullet-}$ is slightly smaller than those of $\mathbf{1b}^{\bullet-}$, the similarities of spin distribution between $\mathbf{2b}^{\bullet+}$ and $\mathbf{1b}^{\bullet+}$ or between $\mathbf{2b}^{\bullet-}$ and $\mathbf{1b}^{\bullet-}$ suggest that HOMO and LUMO of **2b** should also retain a NBMO character to some extent. This NBMO character should be responsible for the small E_1^{sum} value of **2b**.

Table 3. Experimental and theoretical hyperfine coupling constants (in mT) of $\mathbf{2b}^{\bullet+}$ and $\mathbf{2b}^{\bullet-}$

	$\mathbf{2b}^{\bullet+}$[a]		$\mathbf{2b}^{\bullet-}$[b]	
Position	Exptl.	Theor.[c]	Exptl.	Theor.[c]
1, 10	0.227	−0.233	0.214	−0.216
2, 11	0.085[d]	0.066	0.043[e]	0.059
3, 12	0.227	−0.244	0.214	−0.214
5, 8	0.085	0.063	0.056[f]	0.026
6, 7	0.057[f]	0.026	0.157	−0.165
14, 15	0.061[f]	0.016	0.071[f]	0.068

[a] Recorded in CH_2Cl_2 at −70°C. The *g*-value was 2.0025.
[b] Recorded in THF at −30°C. The *g*-value was 2.0024.
[c] Calculated by the HMO–McLachlan method ($\lambda = 1.2$) and the McConnell equation ($Q = -2.4$ mT).[9]
[d] For *d*: 0.013.
[e] For *d*: 0.007.
[f] Assignment may be reversed.

The electronic spectra of the redox species of **2b** exhibits remarkable differences compared to those of **1b** (Table 4). The absorption of $\mathbf{2b}^{\bullet+}$ and $\mathbf{2b}^{\bullet-}$ exhibited many weak and broad bands, and terminated at a relatively shorter-wavelength region. On the other hand, $\mathbf{1b}^{\bullet+}$ and $\mathbf{1b}^{\bullet-}$ gave rise to intense absorptions in considerably long-wavelength regions. The INDO/S calculations for $\mathbf{2a}^{\bullet+}$ and $\mathbf{2a}^{\bullet-}$ indicated that lowest-energy bands (NIR region) should be forbidden transi-

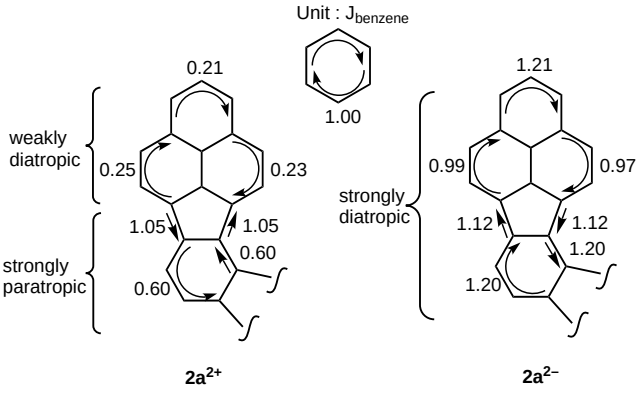

Figure 5. Ring current calculation of $\mathbf{2a}^{2+}$ and $\mathbf{2a}^{2-}$.

Table 4. Maxima, λ_{max} (in nm), of electronic bands for the five redox states of **2b**

$\mathbf{2b}^{2+}/H_2SO_4$	$\mathbf{2b}^{\bullet+}/CH_2Cl_2$	**2b**/Cyclohexane	$\mathbf{2b}^{\bullet-}$/THF	$\mathbf{2b}^{2-}$/THF
419(m)	361(s)	304(m)	280(m)	276(m)
495(m)	469(s)	326(m)	328(m)	320(m)
535(s)	625(m)	352(m)	374(m)	370(m)
664(w)	787(m)	406(s)	514(m)	484(s)
752(w)	880(w)	442(s)	578(s)	520(s)
	1120(w)	496(m)	628(w)	
	1259(w)	572(w)	706(w)	
		618(w)	862(w)	
		658(v.w)	940(v.w)	
		726(v.w)		
		1054(v.w)		
		1242(v.w)		

tions, whereas fully allowed ones for $\mathbf{1a}^{\bullet+}$ and $\mathbf{1a}^{\bullet-}$. The occurrence of many weak and broad absorptions is in line with the lowering of the symmetry ($D_{2h} \rightarrow C_{2v}$), a feature that indicates the change from 'forbidden' to 'allowed' or 'partially allowed' transitions.

The divalent species, $\mathbf{2b}^{2+}$ and $\mathbf{2b}^{2-}$, exhibited relatively simple absorption spectra. However, the assignment of each absorption with the unresolved spectra remains uncertain. The THF solution of $\mathbf{2b}^{2-}$ exhibited a bright orange color and an intense band at 520 nm. These absorptions terminated at the shortest-wavelength among five redox states of **2**. The intense band of $\mathbf{2b}^{2+}$ at 535 nm is flanked on the long-wave side by the weak bands at 550–900 nm, which terminate at longer-wavelength regions than those of $\mathbf{1b}^{2+}$. The INDO/S calculation for $\mathbf{2a}^{2+}$ predicts two nearly degenerate transitions at 593 and 606 nm; the former is due to HOMO (ψ_{15})→LUMO (ψ_{16}) transition and the latter to HOMO (ψ_{15})→NLUMO (ψ_{17}). Although this prediction is also supported by the PPP CI methods, the assignment of the longest wavelength absorption to the HOMO→NLUMO transition remains questionable. However, the small energy differences between S_2 and S_1 states suggest a small gap between ψ_{16} and ψ_{17}, which corresponds to HOMO and LUMO of neutral **2a**, respectively.

Thus, in spite of the differences in the symmetry, **1b** and **2b** were found to behave as four-stage amphoteric redox systems, in which the phenalenyl units played a most important role in exhibiting amphoteric redox properties. Both compounds showed similar properties in the ground-state. However, in the case of mixing a ground state configuration with some excited-state configurations, i.e. ring-currents effect and absorption spectra, the both compounds exhibited largely different properties.

Acknowledgements

This work was supported by a Grant-in-Aid for Scientific research on Priority Areas (No. 06218217) from the Ministry of Education, Culture, Sports, Science and Technology, Japan.

References

1. Ohashi, K.; Kubo, T.; Masui, T.; Yamamoto, K.; Nakasuji, K.; Takui, T.; Kai, Y.; Murata, I. *J. Am. Chem. Soc.* **1998**, *120*, 2018.
2. To evaluate the amphoteric redox abilities of a molecule, the numerical sum (E^{sum}) of the oxidation potential (E^{ox}) and the reduction potential (E^{red}), $E^{sum}=E^{ox}+(-E^{red})$, is used.
3. Spectral data for selected compounds. Acenaphthylene **3**: yellow plates. ^{1}H NMR (270 MHz, $CDCl_3$): δ 7.98 (d, $J=1.0$ Hz, 1H); 7.76 (s, 1H); 7.73 (d, $J=1.0$ Hz, 1H); 6.98 (d, $J=5.1$ Hz, 1H); 6.93 (d, $J=5.1$ Hz, 1H); 2.97 (s, 3H); 1.53 (s, 9H); 1.45 (s, 9H). EI MS m/z 278 (M^+). Acid anhydride **5**: orange powder mp >300°C. ^{1}H NMR (270 MHz, $CDCl_3$): δ 9.41, 9.38, 9.36, 9.32 (s, s, s, s, 2H); 9.03, 9.01, 8.95, 8.88 (s, s, s, s, 2H); 8.29, 8.23 (s, s, 2H); 3.14, 3.12, 3.10 (s, s, s, 6H); 1.80, 1.74, 1.68, 1.67, 1.66, 1.57, 1.53 (s, s, s, s, s, s, s, 36H). FAB MS (NBA) m/z 648 (M^+). IR (KBr) 2961, 1827, 1806, 1764 cm^{-1}. Hydrocarbon **6**: yellow powder mp >300°C. ^{1}H NMR (270 MHz, $CDCl_3$): δ 8.79, 8.71, 8.66 (s, s, s, 2H); 7.82–8.09 (m, 6H); 3.06, 3.05, 3.03 (s, s, s, 6H); 1.76, 1.72, 1.65, 1.63, 1.62, 1.54 (s, s, s, s, s, s, 36H). FAB MS (NBA) m/z 578 (M^+). Anal. calcd for $C_{44}H_{50}$: C, 91.29; H, 8.31. Found: C, 91.15; H, 8.66. Diketone **10**: orange powder ^{1}H NMR (270 MHz, $CDCl_3$): δ 8.87, 8.82, 8.74, 8.69 (s, s, s, s, 2H); 8.26, 8.25, 8.15, 8.13 (s, s, s, s, 2H); 8.02, 7.99, 7.95, 7.93 (s, s, s, s, 2H); 3.88 (t, 4H); 3.21, 3.20, 3.16 (t, t, t, 2H); 1.74, 1.73, 1.72, 1.71, 1.66, 1.63 (s, s, s, s, s, s, s, 36H). FAB MS (NBA) m/z 659 (M^++H). IR (KBr) 2965, 1697 cm^{-1}. Compound **11**: yellow powder. ^{1}H NMR (270 MHz, $CDCl_3$): δ 8.81, 8.76 (s, s, 2H); 8.21, 8.16 (s, s, 2H); 8.03 (s, 2H); 7.61, 7.58 (dt, dt, $J=10.23$, 1.97 Hz, 2H); 6.43, 6.48 (dt, dt, $J=10.23$, 4.62 Hz, 2H); 4.21 (m, $J=1.97$, 4.29 Hz, 2H); 1.76, 1.75, 1.67, 1.65 (s, s, s, s, 36H). FD MS m/z 626 (M^+). Compound **2b**: greenish–brown oil. FD MS m/z 624 (M^+).
4. Nakasuji, K.; Yoshida, K.; Murata, I. *J. Am. Chem. Soc.* **1983**, *105*, 5136.
5. Spiesecke, H.; Schneider, W. G. *Tetrahedron Lett.* **1961**, 468.
6. In a phenalenyl molecule, the position 1,3,4,6,7,9 are called α and 2,5,8 are β. The shift changes ($\Delta\delta_C$) are large (51.8 ppm) at the α position and small (4.9 ppm) at the β position, see: Sethson, I.; Johnels, D.; Edlund, U.; Sygula, A. *J. Chem. Soc., Perkin Trans. 2* **1990**, 1339.
7. (a) London, F. *J. Phys. Radium* **1937**, *8*, 397; (b) Pople, J. A. *Mol. Phys.* **1958**, *1*, 175; (c) McWeeny, R. *Mol. Phys.* **1958**, *1*, 311; (d) Mallion, R. B. *Mol. Phys.* **1973**, *25*, 1415; (e) Aihara, J. *Bull. Chem. Soc. Jpn.* **1985**, *58*, 1045.
8. McLachlan, A. D. *Mol. Phys.* **1960**, *3*, 233.
9. McConnell, H. M. *J. Chem. Phys.* **1956**, *24*, 764.